

1    Recovery of Ammonium from Aqueous Solutions  
2    Using ZSM-5

3    *Michael J. Manto, Pengfei Xie, Mitchell A. Keller, Wilhelm E. Liano, Tiancheng Pu, Chao  
4    Wang\**

5    Department of Chemical and Biomolecular Engineering, Johns Hopkins University, Baltimore,  
6    MD 21218, United States. Email: chaowang@jhu.edu; Fax: +410 516 5510; Tel: +410 516 5843

7  
8    KEYWORDS: *ammonium, nutrient recovery, ZSM-5 zeolites, ion exchange, wastewater*

9     **Abstract.** The demand of reactive nitrogen (N), such as ammonium ( $\text{NH}_4^+$ ) and nitrate ( $\text{NO}_3^-$ ),  
10   continues to increase for fertilizer applications as the population grows, but the Haber Bosch (H-  
11   B) process currently employed for industrial N fixation is challenged by low efficiency and high  
12   energy consumption. Here we report on the investigation of ZSM-5 as a superior sorbent for the  
13   recovery of ammonium from aqueous solutions. Fast capture and release of ammonium ( $\text{NH}_4^+$ )  
14   have been achieved with >90% overall efficiency of recovery using synthetic solutions of  $\text{NH}_4\text{Cl}$   
15   and  $\text{NaCl}$ , respectively. The ZSM-5 sorbent has also been found to be recyclable and sustain high  
16   recovery efficiencies after multiple capture-release cycles. The capture of N has been further  
17   studied systematically in dependence of the dose of sorbent and reaction temperature, based on  
18   which the mechanism, thermodynamics and kinetics of ion exchange are discussed. Compared to  
19   other ion-exchange materials, the ZSM-5 zeolite exhibits superior selectivity for capturing  
20   ammonium in the presence of competing cations ( $\text{NH}_4^+ \gg \text{Ca}^{2+} > \text{Mg}^{2+} > \text{K}^+ > \text{Na}^+$ ) and  
21   demonstrates high efficiency of recovery in real wastewater streams.

22 **1. Introduction**

23 Nitrogen (N) is an essential element for life.<sup>1</sup> Its reactive forms, such as ammonium ( $\text{NH}_4^+$ ) and  
24 nitrate ( $\text{NO}_3^-$ ), are widely applied as fertilizers to promote the growth of plants.<sup>2</sup> Although N  
25 constitutes almost 80% of the terrestrial atmosphere, reactive N is limited in soils and the supply  
26 of biologically accessible N to plants relies on the N fixation from air. Atmospheric dinitrogen  
27 ( $\text{N}_2$ ) can be converted into reactive N by leguminous crops or lightning. Most reactive N today  
28 (>70%) is produced via the artificial chemical synthesis of ammonia ( $\text{NH}_3$ ), i.e., the Haber-Bosch  
29 (H-B) process.<sup>3-4</sup> While the demand of N fertilizers continually escalates with the growing  
30 population, the industrial H-B process is however challenged by the low conversion of  $\text{N}_2$ , high  
31 energy consumption and large carbon footprint.<sup>5-6</sup> This single process accounts for 1-2% of global  
32 energy consumption today, and moreover, the energy efficiency of modern H-B plants is  
33 approaching its theoretical limit.<sup>7</sup>

34 A significant portion (as high as >80% in certain cases<sup>8</sup>) of the reactive N applied to  
35 farmland is lost into water. The runoffs from agriculture as well as other anthropological  
36 discharges from municipal and industrial wastewaters cause the enrichment of reactive N in ponds,  
37 lakes and rivers. This leads to eutrophication, threatening the survival of aquatic species and  
38 jeopardizing sources of clean water.<sup>8-10</sup> Traditionally, chemical precipitation is used to remove  
39  $\text{NH}_4^+$  and other contaminates during wastewater treatment. Although feasible for implementation,  
40 this approach may only be viable for nutrient-rich streams,<sup>11-12</sup> and the struvite derived from direct  
41 chemical precipitation is usually contaminated by toxic substances and not aimed for reuse.<sup>13</sup>  
42 Both the need for tuning the solution pH and the separation of solid products also add expenses  
43 and complexity to the operations.<sup>15-16</sup> For that reason, ion exchange has been extensively studied  
44 for improving the efficiency of nutrients recovery from wastewater<sup>11,17-18</sup>, which can be integrated  
45 with anaerobic digestion<sup>19-20</sup> and/or chemical precipitation<sup>21-22</sup> to produce clean and valuable

46 products. Previous accounts have described the use of commercialized acidic<sup>23-27</sup> and basic<sup>21,28</sup>  
47 resins for cation exchange with dissolved NH<sub>4</sub><sup>+</sup>; however, such sorbents have several  
48 disadvantages, including calcium sulfate fouling in acidic resins, inadvertent adsorption of organic  
49 molecules and organic contamination from the resins. Recent research has turned to zeolites as  
50 alternatives, owing to their structural robustness, tunable and selective adsorption properties,  
51 employment of naturally abundant elements and environmental compatibility.<sup>29-30</sup> Natural zeolites  
52 such as clinoptilolite,<sup>22-23,31-33</sup> wollastonite,<sup>36</sup> sepiolite<sup>37</sup> and others<sup>36,38-39</sup> have been shown to be  
53 effective in capturing the dissolved N from synthetic solutions and wastewater. Some of these  
54 studies have demonstrated controlled release of captured N utilizing acidic<sup>22-23</sup> or basic<sup>36</sup>  
55 regeneration solutions exhibiting ~90 – 100% release for synthetic ion exchange resins<sup>22-23</sup> and  
56 ~45 – 80% release for zeolites.<sup>23,32</sup> However, more effective sorbents with improved capturing  
57 capacity, efficiency of release, and specificity are yet to be developed.<sup>40-41</sup>

58 Here we report on the investigation of ZSM-5 nanocrystals as a sorbent for the recovery of  
59 ammonium from aqueous solutions. Zeolite Socony Mobil-5 (ZSM-5) is an aluminosilicate with  
60 the general chemical formula of Na<sub>n</sub>Al<sub>n</sub>Si<sub>96-n</sub>O<sub>192</sub>-16H<sub>2</sub>O. Isomorphous substitution of Si<sup>4+</sup> by Al<sup>3+</sup>  
61 in the framework induces a negative charge, giving rise to the intrinsic capability for cation  
62 adsorption.<sup>42-43</sup> The kinetics and capacity of NH<sub>4</sub><sup>+</sup> adsorption/desorption on ZSM-5 have been  
63 systematically studied in dependence of the mass loading of sorbent and temperature using  
64 synthetic solutions. The results are fitted into different transport models and isotherms, based on  
65 which the mechanism of NH<sub>4</sub><sup>+</sup> ion exchange is discussed. Finally, the selective capture of  
66 ammonium in the presence of competing cations and from complex media such as real wastewater  
67 are also demonstrated.

68

69

70 **2. Materials and methods**

71 **2.1. Chemicals**

72 Ammonium chloride (NH<sub>4</sub>Cl, ACS grade, VWR), calcium chloride dihydrate (CaCl<sub>2</sub>-2H<sub>2</sub>O, ACS  
73 reagent,  $\geq$  99%), magnesium chloride hexahydrate (MgCl<sub>2</sub>-6H<sub>2</sub>O, ACS reagent, 99.0-102.0%,  
74 Sigma-Aldrich), potassium chloride (KCl, ACS grade, VWR), sodium chloride (NaCl,  $\geq$  99.0%,  
75 Fisher). Deionized water (with a resistance of  $\sim$ 18.2 M $\Omega$ ) was collected from an ELGA PURELAB  
76 flex apparatus.

77 **2.2. Synthesis and characterization of ZSM-5**

78 Commercial NH<sub>4</sub>-ZSM-5 (Alfa Aesar, Si/Al = 11.5) was calcined at 450 °C for 4 h in static air to  
79 convert it into H-ZSM-5, which was used as the sorbent for ion exchange. Scanning electron  
80 microscopy (SEM) images were taken on a JEOL 6700F field emission electron scanning  
81 microscope operated at 10.0 kV. X-ray diffraction (XRD) patterns were obtained from a  
82 PANalytical X'Pert<sup>3</sup> X-ray diffractometer equipped with a Cu K $\alpha$  radiation source ( $\lambda$  = 1.5406 Å).  
83 The Al content was determined by XRF on a Bruker-AXS S4 Explorer. Nitrogen adsorption  
84 measurements were performed on a Micromeritics ASAP 2010 and the samples were degassed  
85 under vacuum for 4 h at 300 °C. Specific surface area (SSA) was calculated according to the  
86 Brunauer-Emmett-Teller (BET) theory.

87 **2.3. Ion exchange**

88 Synthetic solutions of NH<sub>4</sub><sup>+</sup> (containing 1 g of N per litter, or 1 g-N/L, which has a pH of 5.6  $\pm$   
89 0.1) were prepared by dissolving NH<sub>4</sub>Cl in deionized water. A specified amount of ZSM-5 sorbent  
90 was added to 10 mL of this solution and the obtained mixture was stirred at 700 rpm for up to 3 h  
91 for N capture. After the capture, the sorbent was removed from the NH<sub>4</sub>Cl solution by

92 centrifugation and re-dispersed in brine water (10 g-NaCl/L) to release the captured N. At specific  
93 times during the N capture and release processes, aliquots of the reaction solution were extracted  
94 from the mixtures and centrifuged to remove the sorbents. The resulting supernatants were treated  
95 with an indophenol assay<sup>44-45</sup> to determine the concentration of NH<sub>4</sub><sup>+</sup> (see the Supplementary  
96 Material for more details of the assay). Absorption spectra were collected on a Thermo Scientific  
97 GENESYS 10S UV-Vis spectrometer. The amounts of N captured and released were determined  
98 by calculating the difference in N concentration between the initial solution and the collected  
99 supernatants. Various concentrations of NaCl, KCl, CaCl<sub>2</sub> or MgCl<sub>2</sub> were added to the NH<sub>4</sub>Cl  
100 solutions to study the competing cation effect. For wastewater treatment, the activated sludge  
101 (obtained from the Back River Wastewater Treatment Plant in Baltimore, MD) was centrifuged to  
102 remove the solid residues, with the supernatant being used to study the capture of ammonium. The  
103 results presented in the discussion represent the averages of at least three independent repeats.

104 **3. Results and discussion**

105 **3.1. Preparation of ZSM-5 nanocrystals**

106 Commercial NH<sub>4</sub>-ZSM-5 nanocrystals with a Si/Al molar ratio of 11.5 is converted into H-ZSM-  
107 5 via calcination at 450 °C in air.<sup>46-47</sup> Hereby the zeolites are denoted as M-ZSM-5, where M  
108 represents the adsorbed cation (e.g., NH<sub>4</sub><sup>+</sup>, H<sup>+</sup>, Na<sup>+</sup>, etc.). The obtained product has a typical size  
109 of a few hundred nanometers and the particles possess irregular polyhedral shapes (Fig. 1a and b).  
110 The major peaks exhibited in the XRD pattern can be indexed to the MFI type of framework  
111 (JCDPS No. 37-0359), confirming that the crystal structure of the zeolite remains intact during  
112 the sorbent preparation (Fig. 1c). The specific surface area is estimated by the Brunauer–Emmett–  
113 Teller (BET) analysis to be ~376 m<sup>2</sup>/g, which is similar to previously reported results on

114 comparable materials (Fig. 1d).<sup>46-47</sup> The pore volume is calculated to be ~0.163 cm<sup>3</sup>/g by using the  
115 t-plot method.<sup>48</sup>

116 **3.2. N capture and release in synthetic solutions**

117 The capture and release of ammonium (NH<sub>4</sub><sup>+</sup>) are examined using solutions of NH<sub>4</sub>Cl and NaCl,  
118 respectively. Fig. 2a shows a series of UV-Vis spectra collected over the course of N capture. The  
119 NH<sub>4</sub>Cl solution was sampled at different times (0-3 h) and treated with the indophenol assay,<sup>44-45</sup>  
120 resulting in an absorption peak at 640 nm with the intensity proportional to the concentration of  
121 ammonium (see the Supplementary Material for more details of the assay). This peak dissipates as  
122 the time of capture increases, indicating the removal of NH<sub>4</sub><sup>+</sup> from the solution and its uptake by  
123 the ZSM-5 sorbent. Utilizing a pre-established calibration curve (Fig. S1), the concentrations of  
124 residual NH<sub>4</sub><sup>+</sup> in the solution are quantified and are observed to follow the amount of adsorbed N  
125 during the process of capture (Fig. 2b).

126 With the given amount of dissolved N (10 mg), the efficiency of N capture is highly  
127 dependent on the dose of sorbent, with more N captured as dose increases (Fig. 3a). The efficiency  
128 of N capture (the ratio between the captured N and the total amount in the initial solution) varies  
129 from ~44% to ~98% as the applied dose of sorbent increases from 1 to 50 g/L (Fig. 3b). The  
130 dependence of capture efficiency on the loading of sorbent translates into the change of N uptake  
131 with the amount of applied sorbent (Fig. 3c). A maximum uptake of ~440 mg-N/g<sub>zeolite</sub> is observed  
132 when 1 g/L of sorbent is applied, suggesting the potential of the ZSM-5 sorbent for achieving high  
133 capacity of N sorption. N capture via ZSM-5 is also evaluated by varying solution pH in the range  
134 of 5.5 – 9.5. The fraction of N removed decreases at increasing pH (Fig. S2).

135 Release of the captured N is crucial for the recovery of nutrients and for the development  
136 of cost-effective, reusable sorbent materials. To desorb the ammonium anions, the ZSM-5 sorbents

137 are isolated from the NH<sub>4</sub>Cl solution and re-dispersed in a brine solution. The Na<sup>+</sup> cations  
138 exchange with the adsorbed NH<sub>4</sub><sup>+</sup>, and the ammonium released into the brine solution is again  
139 analyzed by using the indophenol assay. Fig. 3e presents the percentages of N (relative to the  
140 captured amount) released during the desorption process using 10 ml of NaCl solution (10 g/L).  
141 Nearly complete release (~92 – 97%) is observed independent of the sorbent dose. By comparing  
142 the time-dependent capture and release (Fig. 3 a and d), it can be seen that the latter exhibits a  
143 flatter curve at the initial stage (e.g., up to 1 h). This observation indicates lower rates of desorption  
144 than adsorption, which will be further elucidated in the following discussion about the kinetics.  
145 Varying the concentration of the NaCl solution used for regeneration (Fig. S2) shows that less N  
146 is released and that the rate of desorption decreases in more diluted solutions. It should be pointed  
147 out that the ammonium may also be released in acidic electrolytes, such as applying HCl and  
148 phosphate to produce (NH<sub>4</sub>)H<sub>2</sub>PO<sub>4</sub> or (NH<sub>4</sub>)<sub>2</sub>HPO<sub>4</sub> which can be used as fertilizers directly.<sup>11,14-15</sup>

149 Recyclability of ZSM-5 is further studied by applying ZSM-5 to successive capture and  
150 release processes in synthetic solutions. Fig. 4a-b show the mass-specific sorption and desorption  
151 of N over 20 capture-release cycles, respectively, using 30 g/L of sorbent. Over the course of the  
152 recyclability analysis from cycle 1 to cycle 20, the capacity of N sorption only dropped slightly  
153 from 30.0 ± 1.0 to 22.8 ± 2.0 mg-N/g<sub>zeolite</sub>. The trend of N desorption exhibits similar behavior,  
154 decreasing from 29.0 ± 1.0 to 16.2 ± 1.2 mg-N/g<sub>zeolite</sub>. These results demonstrate that the ZSM-5  
155 zeolite can be reused for multiple capture-release cycles, which is an important merit of cost-  
156 effective sorbents for practical applications.

157 It is interesting to notice the rather consistent trends of N sorption and desorption from the  
158 recyclability studies (Fig. 4a-b). This finding suggests that the recyclability of the ZSM-5 sorbent  
159 may be mainly limited by the release of captured N, which is better visualized by the overlapped

160 trends of release and recovery efficiencies over the course of the capture-release cycles (Fig. 4c).  
161 The release efficiency represents the ratio between the released and the captured N, while the  
162 recovery efficiency refers to the net percentage of the N recovered per capture-release cycle from  
163 the NH<sub>4</sub>Cl solution. It is found that the two efficiencies exhibit similar trends depending on the  
164 number of cycles, with the release efficiency dropping from ~97% to ~71% and the recovery  
165 efficiency from ~90% to ~68% throughout the 20 cycles. It is thus postulated that some ammonium  
166 cations get trapped within the pores of ZSM-5 (due to, for example, hydrogen bonding between  
167 NH<sub>4</sub><sup>+</sup> and the framework oxygen<sup>49-51</sup>) during release and block the active sites for cation adsorption  
168 in the successive adsorption, causing the loss of uptake capacity.

169 **3.3. Kinetics of ammonium sorption**

170 The capture of N was further carried out at different temperatures to investigate the kinetics of  
171 ammonium sorption. This was done by applying 30 g/L of ZSM-5 sorbent to 10 mL of NH<sub>4</sub>Cl  
172 solution (1 g-N/L) at 5 – 95 °C. Fig. 5a presents the dependence of N sorption on time at the  
173 various temperatures. The time-dependent sorption consistent exhibits a three-stage behavior,  
174 namely a rapid increase during the initial ~15 min, followed by a leveling-off regime, and then a  
175 plateau at time beyond. Throughout the capturing process, higher capacities of sorption were  
176 observed at higher temperatures. Noticeably, it took less time to reach the equilibrium, as indicated  
177 by the plateau in the sorption curves, at a higher temperature, e.g., <1 h at 95 °C versus ~2 h at 5  
178 °C (Fig. 5a). The equilibrium uptake was also found to increase slightly as the temperature was  
179 raised, which suggests shift of equilibrium for the ion exchange reaction (see the following  
180 discussion).

181 The three-stage behavior observed in the sorption kinetics is indicative of a diffusion-  
182 controlled process during the N capture.<sup>52-53</sup> The two kinetic regimes observed in sorption with

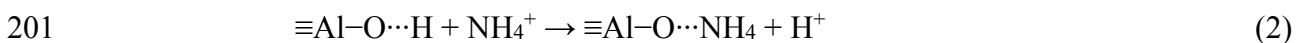
183 rapid increase and leveling-off can be ascribed to film and pore diffusion, respectively (Fig. 5a).  
184 According to the intra-particle diffusion (IPD) model,<sup>54-56</sup> the time-dependent sorption ( $Q_t$ ) can be  
185 fit by the following equation

186 
$$Q_t = kt^{0.5} + C \quad (1)$$

187 Fig. 5b shows the comparison of fitted pore ( $k_p$ ) and film ( $k_f$ ) diffusion coefficients at the  
188 various temperatures. For all the temperatures of capture,  $k_p$  is generally much smaller than  $k_f$ ,  
189 indicating that the diffusion through the micropores within the zeolites is limiting the rate of  
190 sorption. It is interesting to find that, while  $k_f$  increases with temperature,  $k_p$  exhibits rather weak  
191 (or even negative) dependence on temperature. The former is typical for molecular diffusion in  
192 liquid phase and consistent with the previously reported cation diffusion in zeolites.<sup>57-58</sup> The latter  
193 phenomenon is likely a result of the Knudsen diffusion of ammonium through the micropores of  
194 zeolites, which could exhibit lower diffusion coefficient at higher temperatures due to the  
195 enhancement of Brownian motion and increase of collisions between the ions and the zeolite  
196 framework.<sup>59-62</sup>

197 **3.4. Ion-exchange mechanism**

198 Cation exchange on zeolites is generally believed to be associated with the Brønsted acid sites  
199 introduced by the substitution of  $\text{Si}^{4+}$  by  $\text{Al}^{3+}$ .<sup>29,43,63</sup> When H-ZSM-5 is used for N capture, the ion-  
200 exchange reaction can be written as (Scheme 1)



202 This reaction is associated with the release of protons to the solution, as confirmed by the observed  
203 change of solution pH from 5.6 to 3.5 during the first capture step of the recyclability study (Table  
204 1). In the subsequent capture and release cycles, the ion exchange involves  $\text{Na}^+$  and the reaction  
205 can be written as (Scheme 1).



207 Again, this reaction is confirmed by the measured changes of solution pH, i.e., decreasing from  
208 6.9 to 5.7 – 5.8 after the release of ammonium into the NaCl solution and increasing from 5.6 to  
209 6.7 after the capture of ammonium from the NH<sub>4</sub>Cl solution (Table 1). It is noticed that silanol  
210 groups may be present on ZSM-5 and also contribute to cation exchange,<sup>64</sup> but that mechanism is  
211 unlikely to play a significant role in the present study carried out in acidic or neutral solutions, as  
212 also suggested by the observation of lower N capture efficiency at increasing solution alkalinity  
213 (Fig. S2).

However, it is necessary to point out that the molar ratio between the captured N and the number of Al sites present in the sorbent can go beyond one. The dose-dependent studies (Fig. 3c) shows that the N/Al ratio increases as the amount of applied sorbent is reduced and goes above 1 at the doses of <30 g/L (for the given 10 mL of NH<sub>4</sub>Cl solution with 1 g-N/L). The cation exchangeable capacity (CEC) of the ZSM-5 sorbent was estimated to be ca. 1.45 mmol/g<sub>zeolite</sub>, based on the X-ray fluorescence (XRF) analysis<sup>65</sup> of Na-ZSM-5 with H<sup>+</sup> completely substituted by Na<sup>+</sup> (comparable with the previously reported value for this material<sup>66</sup>). Thereby the observation of much higher uptake of ammonium than the CEC on the ZSM-5 sorbent is likely also a result of the formation of hydrogen bond between NH<sub>4</sub><sup>+</sup> and the framework oxygen,<sup>49-51</sup> which could have trapped extra NH<sub>4</sub><sup>+</sup> cations in the micropores of the zeolite during the capturing process. As mentioned above, it is postulated that the same mechanism caused the capacity degradation observed in the recyclability studies.

226 Fitting the capacity of sorption,  $Q_{\text{eq}}$ , and residual concentration of N,  $C_{\text{eq}}$ , at equilibrium  
 227 with isotherms enables further corroboration of the N sorption mechanism.<sup>23,33-34,39-41</sup> Fig. 6b  
 228 presents the isotherm derived from the mass loading-dependent capturing experiments carried out

229 at room temperature, with the parameters used for fitting summarized in Table 2. It can be seen  
230 that the Langmuir isotherm, associated with monolayer adsorption, only fits well when the  
231 equilibrium concentration ( $C_{eq}$ ) is low, e.g., <200 mg-N/L, which is corresponding to the regime  
232 with  $N/Al \approx 1$  at high sorbent doses (e.g., >30 g/L in Fig. 6a). In the high- $C_{eq}$  regime, the Freundlich  
233 and Redlich-Peterson isotherms outperform the Langmuir isotherm in fitting. Overall, the Redlich-  
234 Peterson isotherm, considered a hybrid approach derived from both of the Langmuir and  
235 Freundlich isotherms and other sorbate-sorbate interactivity principles, exhibits the best fitting to  
236 the experimental data ( $R^2 = 0.957$ ).<sup>39</sup> This suggests that a hybrid monolayer-multilayer behavior  
237 occurs, with the distribution dependent on the equilibrium concentration of ammonium, namely  
238 more Langmuir-type of adsorption at low concentrations and multilayer-dominant situation at high  
239 concentrations. This finding is well in line with the above analysis derived from the N/Al ratios.

240 **3.5. N capture and release in complex media**

241 After studying the N capture and release in synthetic solutions, we aim to further demonstrate the  
242 potential application of the zeolite sorbent for N recovery in practical conditions. For that purpose,  
243 the ZSM-5 sorbent was applied to capture ammonium from synthetic solutions in the presence of  
244 competing cations and recovery of ammonium from real wastewater containing a bevy of inorganic  
245 and organic impurities.

246 Previously, the effects of coexisting cations have been extensively studied in the ion  
247 exchange for N recovery, with the primary focus placed on the competing adsorption of  $Na^+$ ,  $K^+$ ,  
248  $Ca^{2+}$ ,  $Mg^{2+}$  etc. that are commonly present in wastewater.<sup>23-24,31,33,38-39,41</sup> To examine these effects  
249 on the capture of N using ZSM-5, 20 – 100 mmol/L of  $Na^+$ ,  $K^+$ ,  $Ca^{2+}$  and  $Mg^{2+}$  were added to the  
250 NH<sub>4</sub>Cl solution (1 g-N/L or 71.4 mmol-N/L), and the capacity of N sorption was measured at the  
251 various cation concentrations (Fig. 7a). It was found that introduction of these cations had

252 insignificant impact on the capacity of N sorption at relatively low concentrations. At equimolar  
253 or higher concentrations of cations, the capacity had ~10 – 15% of drop, with  $\text{Ca}^{2+}$  exhibiting the  
254 largest impact. From the results about competing cations, it can be derived that the affinity to the  
255 ZSM-5 sorbent follows the trend:  $\text{NH}_4^+ \gg \text{Ca}^{2+} > \text{Mg}^{2+} > \text{K}^+ > \text{Na}^+$ . The observed trend for metal  
256 cations is consistent with the calculated binding energies of metal cations on ZSM-5,<sup>67</sup> whereas  
257 the much stronger affinity of ammonium could also be attributed to the formation of hydrogen  
258 bond with the framework oxygen.<sup>49-51</sup> It is noticed that the overall order of ion exchange observed  
259 on ZSM-5 differs from those reported on natural zeolites (e.g.,  $\text{K}^+ > \text{NH}_4^+ > \text{Ba}^{2+} > \text{Na}^+ > \text{Ca}^{2+}$  on  
260 clinoptilolite).<sup>29</sup> This difference can be attributed to the unique framework structure of ZSM-5 and  
261 thus highlights the superiority of using ZSM-5 as sorbent for N recovery.

262 Real wastewater contains a wide range of organic and biomolecular contaminants in  
263 addition to competing ions. (Bio)fouling caused by these contaminants has been recognized to be  
264 one of the major challenges for the applications of ion-exchange sorbents for wastewater  
265 treatment.<sup>29,63</sup> To demonstrate its potential for practical applications, the ZSM-5 sorbent has been  
266 used to recover N from the anaerobic digestion effluents obtained from the Back River Wastewater  
267 Treatment Plant in Baltimore, MD. After removing the sludge by centrifugation, the supernatant  
268 was analyzed to contain ~38.4 mg of dissolved ammonium per liter. The ZSM-5 sorbent achieved  
269 91% of capture efficiency and 89% of release efficiency, corresponding to an overall efficiency of  
270 ~90% for N recovery from this solution (Fig. 7b). Moreover, the ZSM sorbent was also found to  
271 be capable of sustaining the high recovery efficiencies throughout multiple capture-release cycles  
272 for the wastewater solutions. The recovery efficiency dropped by merely <10% over five cycles,  
273 indicating that ZSM-5 is potentially resistant to fouling by the organic and biomolecular  
274 impurities.

275 **4. Conclusion**

276 We have investigated ZSM-5 as sorbent for the recovery of ammonium from aqueous solutions.  
277 Fast capture and release of ammonium ( $\text{NH}_4^+$ ) have been achieved with >90% overall efficiency  
278 of recovery using synthetic solutions of  $\text{NH}_4\text{Cl}$  and  $\text{NaCl}$ , respectively. The ZSM-5 sorbent has  
279 also been shown to be recyclable and sustain high recovery efficiencies after multiple capture-  
280 release cycles. Systematic studies of the N sorption process at different mass loadings of sorbent  
281 and reaction temperatures reveal hybrid mono- and multi-layer adsorption, with the distribution  
282 between these two models depending on the equilibrium concentration of ammonium, and  
283 diffusion-controlled kinetic performance, with the Knudsen diffusion of ammonium through the  
284 micropores of zeolites identified to be the rate-limiting factor. Moreover, the ZSM-5 sorbent has  
285 been demonstrated to be selective for capturing ammonium in the presence of competing cations,  
286 with the affinity following the order  $\text{NH}_4^+ \gg \text{Ca}^{2+} > \text{Mg}^{2+} > \text{K}^+ > \text{Na}^+$ , and efficient in recovering  
287 ammonium from real wastewater streams. Our work highlights the great potential of synthetic  
288 zeolites as sorbents for efficient recovery of valuable nutrients from wastewater and other aqueous  
289 solutions.

290 **Conflicts of interest**

291 There are no conflicts of interest to declare.

292 **Acknowledgements**

293 This work is supported by the National Science Foundation (CHE-1664967). We thank Dr. Edward  
294 J. Bouwer and his research group for providing the wastewater samples.

295 **Scheme 1.** Proposed ion exchange mechanism for N recovery.

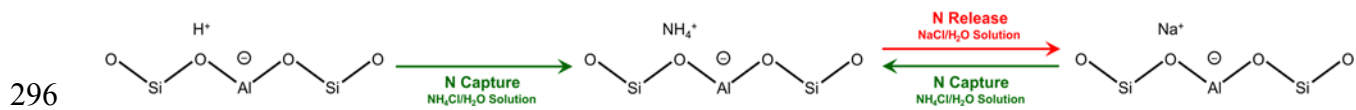
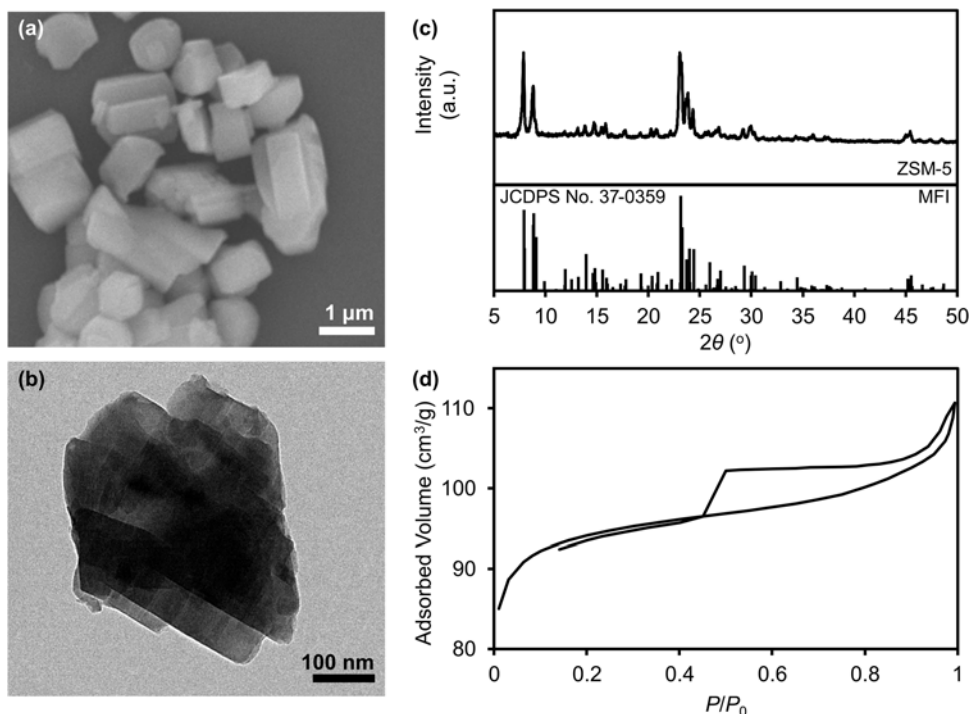


**Table 1.** Measured solution pH during initial and subsequent capture and release cycles.

Cycle	Solution	Stage	pH
First Capture-Release Cycle	NH <sub>4</sub> Cl/H <sub>2</sub> O	Before Capture	5.6 ± 0.1
		After Capture	3.5 ± 0.1
	NaCl/H <sub>2</sub> O	Before Release	6.9 ± 0.1
		After Release	5.7 ± 0.1
Subsequent Capture-Release Cycles	NH <sub>4</sub> Cl/H <sub>2</sub> O	Before Capture	5.6 ± 0.1
		After Capture	6.7 ± 0.1
	NaCl/H <sub>2</sub> O	Before Release	6.9 ± 0.1
		After Release	5.8 ± 0.1

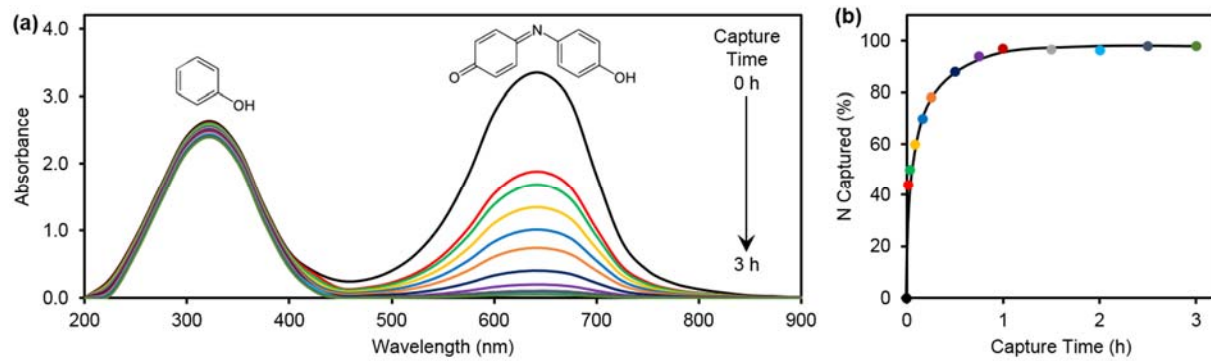
**Table 2.** Equations and fitting parameters of the N sorption isotherms.

Isotherm	Equation	Parameters		Coefficient of Determination ( $R^2$ )	
Langmuir	$Q_{eq} = \frac{Q_m K_L C_{eq}}{1 + K_L C_{eq}}$	$K_L$ 0.00588 L/mg-N	$Q_m$ 161.3 mg-N/g	0.864	
Freundlich	$Q_{eq} = K_F C_{eq}^n$	$K_F$ 0.651	$n$ 0.994	0.944	
Redlich-Peterson	$Q_{eq} = \frac{a C_{eq}}{1 + b C_{eq}^n}$	$a$ 0.801	$b$ 0.051	$n$ 0.021	0.957



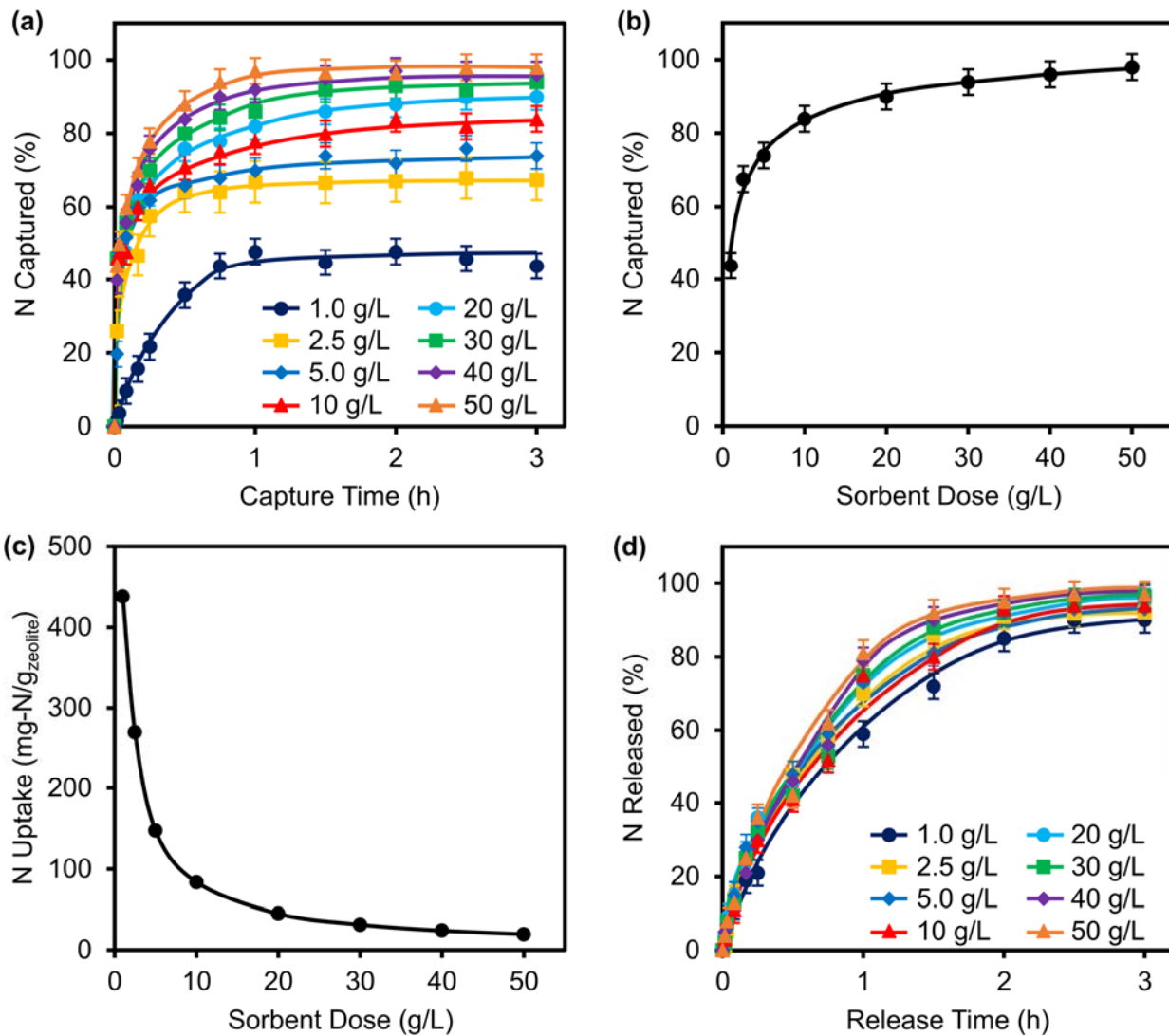
301

302 **Fig. 1.** (a) SEM and (b) TEM images of ZSM-5 nanocrystals. (c) XRD pattern of the as-prepared  
 303 ZSM-5 compared to the MFI framework. (d) Measured N<sub>2</sub> adsorption profile for ZSM-5.



304

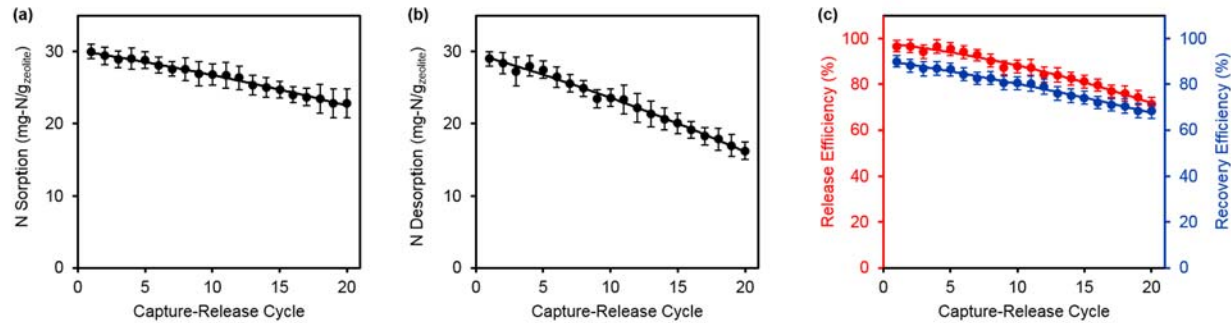
305 **Fig. 2.** (a) Typical UV-Vis spectra collected over the course of N capture using the indophenol  
 306 blue assay. (b) Time-dependent N capture efficiency of the ZSM-5 sorbent (50 g/L in 1 g-N/L  
 307 NH<sub>4</sub>Cl) derived from the spectra shown in (a).



308

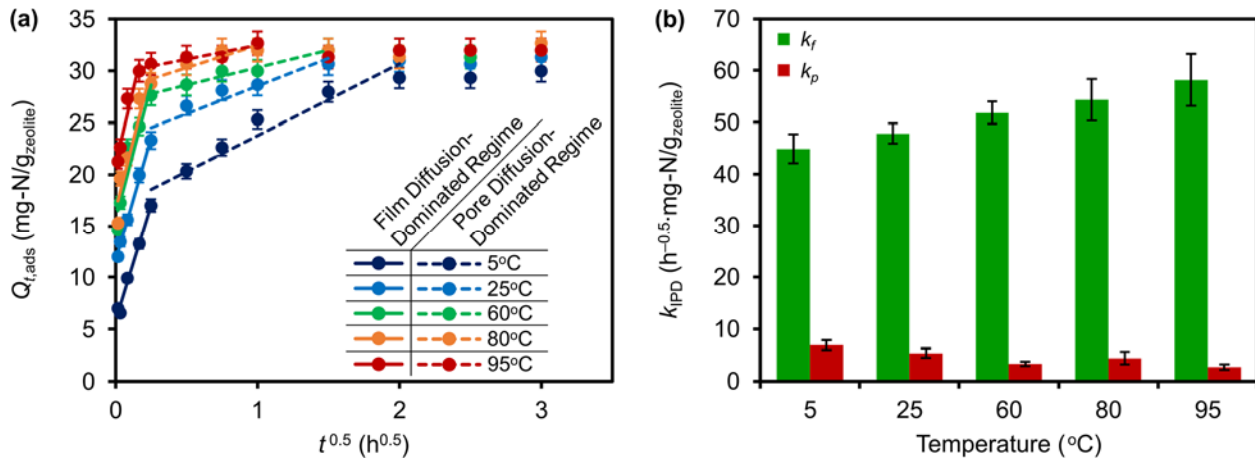
309 **Fig. 3.** Dependence of N capture and release on the dose of sorbent: (a) Time-dependent capture,  
 310 (b) achieved efficiency of N capture at equilibrium, (c) calculated capacity of N sorption and (d)  
 311 time-dependent release.

312



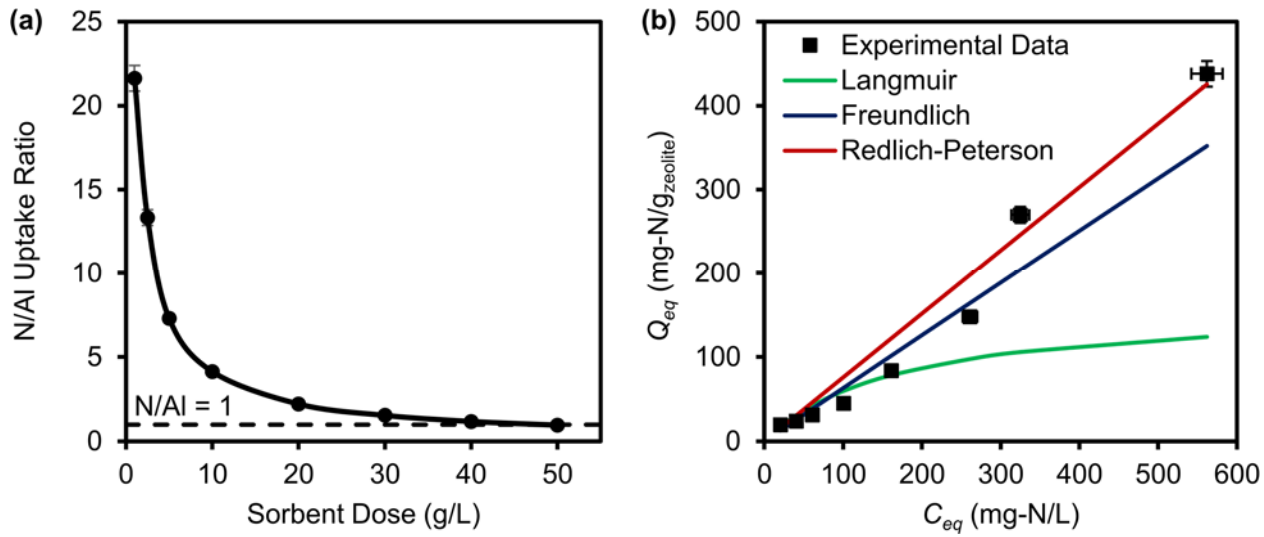
313

314 **Fig. 4.** Recyclability of the ZSM-5 sorbent for N recovery using 30 g/L of sorbent: (a) Capacity of  
 315 N sorption and (b) desorption over 20 capture-release cycles. (c) Overlapped trends of release and  
 316 recovery efficiencies throughout the capture-release cycles.

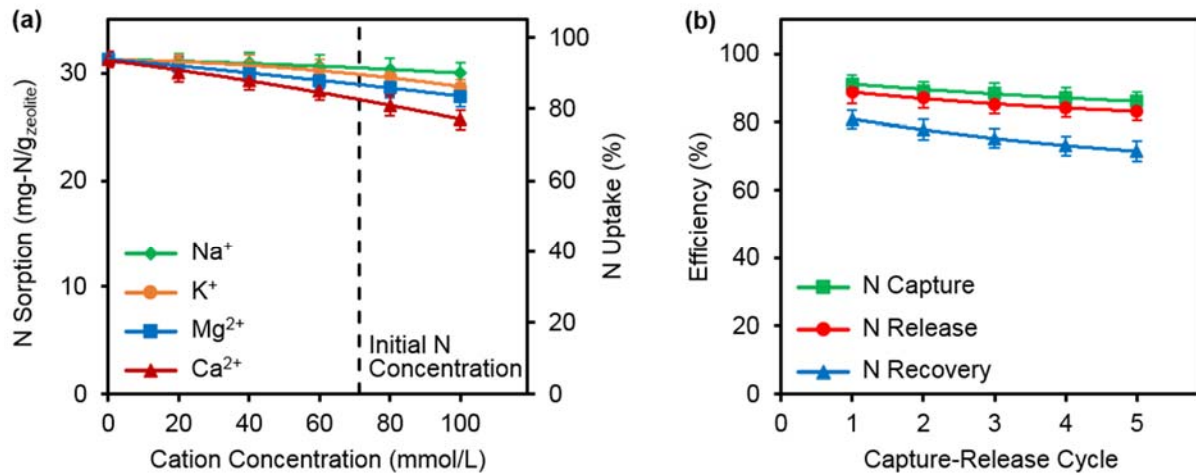


317

318 **Fig. 5.** (a) Time-dependent sorption at various temperatures (with 30 g/L of sorbent), with the  
 319 fitted film ( $k_f$ ) and pore ( $k_p$ ) diffusion coefficients using the intra-particle diffusion model  
 320 summarized in (b).



321 **Fig. 6.** (a) Calculated N/Al ratio for the N sorption at the various doses of sorbent. (b) Fitting for  
 322 the measured equilibrium concentrations ( $C_{eq}$ ) and uptake ( $Q_{eq}$ ) with the three types of isotherms.  
 323



324

325 **Fig. 7.** (a) Using ZSM-5 for N capture in the presence of competing cations. (b) Efficiencies of N  
 326 capture, release and recovery from a real wastewater stream (containing 38.4 mg-N/L) by using  
 327 the ZSM-5 sorbent. The dose of sorbent is at 30 g/L in all cases.

328 **Table of Contents Graphic**



329

330

331 **References**

332 (1) Greenwood, N. N.; Earnshaw, A. In *Chemistry of the Elements*, 2nd ed; Butterworth-  
333 Heinemann: Oxford, 1997; Chapter 22, pp 1341.

334 (2) Black, C. A. In *Soil-Plant Relationships*, 2nd ed; Kriger, R.E., Eds.; Malabar: FL, 1984;  
335 Chapter 7, pp 792.

336 (3) Smil, V. Detonator of the population explosion. *Nature* **1999**, *400*, 415-415.

337 (4) Bodirsky, B. L.; Popp, A.; Lotze-Campen, H.; Dietrich, J. P.; Rolinski, S.; Weindl, I.;  
338 Schmitz, C.; Muller, C.; Bonsch, M.; Humpenoder, F.; Biewald, A.; Stevanovic, M. *Nat.*  
339 *Commun.* **2014**, *5*, 3858.

340 (5) Smil, V. *Enriching the Earth: Fritz Haber, Carl Bosch, and the Transformation of World*  
341 *Food Production*; MIT Press: Boston, 2004.

342 (6) Cherkasov, N.; Ibhadon, A. O.; Fitzpatrick, P. A review of existing and alternative methods  
343 for greener nitrogen fixation. *Chem. Eng. Process.* **2015**, *90*, 24-33.

344 (7) Matassa, S.; Batstone, D. J.; Hulsen, T.; Schnoor, J.; Verstraete, W. Can Direct Conversion  
345 of Used Nitrogen to New Feed and Protein Help Feed the World? *Environ. Sci. Technol.*  
346 **2015**, *49*, 5247-5254.

347 (8) Lewis, W. M.; Wurtsbaugh, W. A.; Paerl, H. W. Rationale for control of anthropogenic  
348 nitrogen and phosphorus to reduce eutrophication of inland waters. *Environ. Sci. Technol.*  
349 **2011**, *45*, 10300-10305.

350 (9) Elser, J. J.; Bracken, M. E. S.; Cleland, E. E.; Gruner, D. S.; Harpole, W. S.; Hillebrand H.;  
351 Ngai, J. T.; Seabloom, E. W.; Shurin, J. B.; Smith, J. E. Global analysis of nitrogen and  
352 phosphorus limitation of primary producers in freshwater, marine and terrestrial ecosystems.  
353 *Ecol. Lett.*, **2007**, *10*, 1135-1142.

354 (10) Tilman, D.; Fargione, J.; Wolff, B.; D'Antonio, C.; Dobson, A.; Howarth, R.; Schindler, D.;  
355 Schlesinger, W. H.; Simberloff, D.; Swackhamer, D. Forecasting agriculturally driven global  
356 environmental change. *Science*, **2001**, *292*, 281-284.

357 (11) Liu, Y. H.; Kwag, J. H.; Kim, J. H.; Ra, C. S. Recovery of nitrogen and phosphorus by  
358 struvite crystallization from swine wastewater. *Desalination*, **2011**, *277*, 364-369.

359 (12) Kumar, R.; Pal, P. Assessing the feasibility of N and P recovery by struvite precipitation  
360 from nutrient-rich wastewater: a review. *Environ. Sci. Pollut. Res.*, **2015**, *22*, 17453-17464.

361 (13) Mehta, C. H.; Khunjar, W. O.; Nguyen, V.; Tait, S.; Batstone, D. J. Technologies to Recover  
362 Nutrients from Waste Streams: A Critical Review. *Crit. Rev. Environ. Sci. Technol.* **2015**,  
363 *45*, 385-427.

364 (14) Darwish, M.; Aris, A.; Puteh, M. H.; Abideen, M. Z.; Othman, M. N. Ammonium-Nitrogen  
365 Recovery from Wastewater by Struvite Crystallization Technology. *Sep. Purif. Rev.*, **2016**,  
366 *45*, 261-274.

367 (15) Doyle, J. D.; Parsons, S. A., Struvite formation, control and recovery. *Water Res*, **2002**, *36*,  
368 3925-3940.

369 (16) Batstone, D. J.; Hulsen, T.; Mehta, C. M.; Keller, J. *Chemosphere*, **2015**, *140*, 2-11.

370 (17) Hedstrom, A. Ion Exchange of Ammonium in Zeolites: A Literature Review. *J. Environ.*  
371 *Eng.* **2001**, *127*, 673-681.

372 (18) Beaton, A. D.; Wadham, J. L.; Hawkings, J.; Bagshaw, E. A.; Lamarche-Gagnon, G.;  
373 Mowlem, M. C.; Tranter, M. High-Resolution in Situ Measurement of Nitrate in Runoff from  
374 the Greenland Ice Sheet. *Environ. Sci. Technol.* **2017**, *51*, 12518-12527.

375 (19) Gao, H.; Scherson, Y. D.; Wells, G. F. Towards energy neutral wastewater treatment:  
376 methodology and state of the art. *Environ. Sci. Process. Impact*, **2014**, *16*, 1223-1246.

377 (20) Amini, A.; Aponte-Morales, V.; Wang, M.; Dilbeck, M.; Lahav, O.; Zhang, Q.; Cunningham,  
378 J. A.; Ergas, S. J. Cost-effective treatment of swine wastes through recovery of energy and  
379 nutrients. *Waste Manag.*, **2017**, *69*, 508-517

380 (21) Liberti, L.; Boari, G.; Petruzzelli, D.; Passino, R. Nutrient removal and recovery from  
381 wastewater by ion exchange. *Water Res.* **1981**, *15*, 337-342.

382 (22) Lind, B.; Ban, Z.; Byden, S. Nutrient recovery from human urine by struvite crystallization  
383 with ammonia adsorption on zeolite and wollastonite. *Bioresource Technol.* **2000**, *73*, 167-  
384 174.

385 (23) Tarpeh, W. A.; Udert, K. A.; Nelson, K. L. Comparing Ion Exchange Adsorbents for  
386 Nitrogen Recovery from Source-Separated Urine. *Environ. Sci. Technol.* **2017**, *51*, 2373-  
387 2381.

388 (24) Wirthensohn, T.; Waeger, F.; Jelinek, L.; Fuchs, W. Ammonium removal from anaerobic  
389 digester effluent by ion exchange. *Water Sci. Technol.* **2009**, *60*, 201-210.

390 (25) Mumford, K. A.; Northcott, K. A.; Shallcross, D. C.; Snape, I.; Stevens, G. W. Comparison  
391 of Amberlite IRC-748 Resin and Zeolite for Copper and Ammonium Ion Exchange. *J. Chem.*  
392 *Eng. Data* **2008**, *53*, 2012-2017.

393 (26) Gefeniene, A.; Kauspediene, D.; Snukiskis, J. Performance of sulphonated cation exchangers  
394 in the recovery of ammonium from basic and slight acidic solutions. *J. Hazard.*  
395 *Mater.* **2006**, *135*, 180-187.

396 (27) Ancuta, A.; Kauspediene, D.; Gefeniene, A.; Snukiskis J.; Vasileviciute, E. Effect of  
397 hydroxyl and nitrate ions on the sorption of ammonium ions by sulphonated cation  
398 exchangers. *Desalination* **2005**, *175*, 259-268.

399 (28) Leakovic, S.; Mijatovic, I.; Cerjan-Stefanovic, S.; Hodzic, E. Nitrogen removal from  
400 fertilizer wastewater by ion exchange. *Water Res.* **2000**, *34*, 185-190.

401 (29) Wang, S.; Peng, Y. Natural zeolites as effective adsorbents in water and wastewater  
402 treatment. *Chem. Eng. J.* **2010**, *156*, 11-24.

403 (30) Ali, I.; Asim, M.; Khan, T. A. Low cost adsorbents for the removal of organic pollutants  
404 from wastewater *J. Environ. Manage.* **2012**, *113*, 170-183.

405 (31) Erbil, A. C.; Soyer E.; Beler-Baykal, B. Ammonium Ion Removal with a Natural Zeolite in  
406 Monodispersed and Segregated Fluidized Beds. *Ind. Eng. Chem Res.* **2011**, *50*, 6391-6403.

407 (32) Beler-Baykal, B.; Allar, A. D.; Bayram, S. Nitrogen recovery from source-separated human  
408 urine using clinoptilolite and preliminary results of its use as fertilizer. *Water Sci.*  
409 *Technol.* **2011**, *63*, 811-817.

410 (33) Guo, X.; Zeng, L.; Li, X.; Park, H. Ammonium and potassium removal for anaerobically  
411 digested wastewater using natural clinoptilolite followed by membrane pretreatment. *J.*  
412 *Hazard. Mater.* **2008**, *151*, 125-133.

413 (34) Karadag, D.; Koc, Y.; Turan, M.; Ozturk, M. A comparative study of linear and non-linear  
414 regression analysis for ammonium exchange by clinoptilolite zeolite. *J. Hazard.*  
415 *Mater.* **2007**, *144*, 432-437.

416 (35) Wen, D.; Ho, Y.; Tang, X. Comparative sorption kinetic studies of ammonium onto  
417 zeolite. *J. Hazard. Mater.* **2006**, *133*, 252-256.

418 (36) Lind, B.; Ban, Z.; Byden, S. Nutrient recovery from human urine by struvite crystallization  
419 with ammonia adsorption on zeolite and wollastonite. *Bioresource Technol.* **2000**, *73*, 167-  
420 174.

421 (37) Balci, S.; Dincel, Y. Ammonium ion adsorption with sepiolite: use of transient uptake  
422 method. *Chem. Eng. Process.* **2002**, *41*, 79-85.

423 (38) Karapinar, N. Application of natural zeolite for phosphorus and ammonium removal from  
424 aqueous solutions. *J. Hazard. Mater.* **2009**, *170*, 1186-1191.

425 (39) Lei, L.; Li, X.; Zhang, X. Ammonium removal from aqueous solutions using microwave-  
426 treated natural Chinese zeolite. *Sep. Purif. Technol.* **2008**, *58*, 359-366.

427 (40) Zhang, B.; Wu, D.; Wang, C.; He, S.; Zhang Z.; Kong, H. Simultaneous Removal of  
428 Ammonium and Phosphate by Zeolite Synthesized From Coal Fly Ash as Influenced by Acid  
429 Treatment. *J. Environ. Sci.-China* **2007**, *19*, 540-545.

430 (41) Thornton, A.; Pearce, P.; Parsons, S. A. Ammonium removal from solution using ion  
431 exchange on to MesoLite, an equilibrium study. *J. Hazard. Mater.* **2007**, *147*, 883-889.

432 (42) Manto, M. J.; Xie, P.; Keller, M. A.; Liano, W. E.; Pu, T.; Wang, C. Recovery of Inorganic  
433 Phosphorus Using Copper-Substituted ZSM-5. *ACS Sustainable Chem. Eng.* **2017**, *5*, 6192-  
434 6200.

435 (43) Chu, P.; Dwyer, F. G. In *Intrazeolite Chemistry*, 1st ed; Stucky, G. D.; Dwyer, F. G., Eds.;  
436 American Chemical Society: Washington, D.C., 1983; Chapter 4, pp 59-78.

437 (44) Solorzano, L. Determination of Ammonia in Natural Waters by the Phenolhypochlorite  
438 Method. *Limnol. Oceanogr.* **1969**, *14*, 799-801.

439 (45) Weatherburn, M. W. Phenol-hypochlorite reaction for determination of ammonia. *Anal.*  
440 *Chem.* **1967**, *39*, 971-974.

441 (46) Bleken, F.; Skistad, W.; Barbera, K.; Kustova, M.; Bordiga, S.; Beato, P.; Lillerud, K. P.;  
442 Svelle, S.; Olsbye, U. Conversion of methanol over 10-ring zeolites with differing volumes

443 at channel intersections: comparison of TNU-9, IM-5, ZSM-11 and ZSM-5. *Phys. Chem.*  
444 *Chem. Phys.* **2011**, *13*, 2539–2549.

445 (47) Kustova, M. Y.; Rasmussen, S. B.; Kustov, A. L.; Christensen, C. H. Direct NO  
446 decomposition over conventional and mesoporous Cu-ZSM-5 and Cu-ZSM-11 catalysts:  
447 Improved performance with hierarchical zeolites. *Appl. Catal., B* **2006**, *67*, 60–67.

448 (48) Xie, P.; Luo, Y.; Ma, Z.; Huang, C.; Miao, C.; Yue, Y.; Hua, W.; Gao, Z. Catalytic  
449 decomposition of N<sub>2</sub>O over Fe-ZSM-11 catalysts prepared by different methods: Nature of  
450 active Fe species. *J. Catal.* **2015**, *330*, 311–322.

451 (49) Ye, L.; Lo, B. T. W.; Qu, J.; Wilkinson, I.; Hughes, T.; Murray, C. A.; Tang, C. C.; Tsang,  
452 S. C. E. Probing atomic positions of adsorbed ammonia molecules in zeolite. *Chem.*  
453 *Commun.* **2016**, *52*, 3422-3425.

454 (50) Krishna, R.; van Baten, J. M. Hydrogen Bonding Effects in Adsorption of Water-Alcohol  
455 Mixtures in Zeolites and the Consequences for the Characteristics of the Maxwell-Stefan  
456 Diffusivities. *Langmuir* **2010**, *26*, 10854-10867.

457 (51) Wakabayashi, F.; Kondo, J. N.; Domen, K.; Hirose, C. FT-IR Study of H<sub>2</sub><sup>18</sup>O Adsorption on  
458 H-ZSM-5: Direct Evidence for the Hydrogen-Bonded Adsorption of Water. *J. Phys. Chem.*  
459 **1996**, *100*, 1442-1444.

460 (52) Onyango, M. S.; Kuchar, D.; Kubota, M.; Matsuda, H. Adsorptive Removal of Phosphate  
461 Ions from Aqueous Solution Using Synthetic Zeolite. *Ind. Eng. Chem. Res.* **2007**, *46*,  
462 894–900.

463 (53) He, Y.; Lin, H.; Dong, Y.; Liu, Q.; Wang, L. Simultaneous removal of ammonium and  
464 phosphate by alkaline-activated and lanthanum-impregnated zeolite. *Chemosphere* **2016**,  
465 *164*, 387–395.

466 (54) Simonin, J. On the comparison of pseudo-first order and pseudo-second order rate laws in  
467 the modeling of adsorption kinetics. *Chem. Eng. J.* **2016**, *300*, 254-263.

468 (55) Rudzinski, W.; Plazinski, W. Theoretical description of the kinetics of solute adsorption at  
469 heterogeneous solid/solution interfaces: On the possibility of distinguishing between the  
470 diffusional and the surface reaction kinetics models. *Appl. Surf. Sci.* **2007**, *253*, 5827-5840.

471 (56) Boyd, G. E.; Adamson, A. W.; Myers, L. S. The Exchange Adsorption of Ions from Aqueous  
472 Solutions by Organic Zeolites. II. Kinetics. *J. Am. Chem. Soc.* **1947**, *67*, 2836-2848.

473 (57) Kärger, J.; Ruthven, D. M. Diffusion in nanoporous materials: fundamental principles,  
474 insights and challenges. *New J. Chem.* **2016**, *40*, 4027-4048.

475 (58) Dyer, A.; White, K. J. Cation diffusion in the natural zeolite clinoptilolite. *Thermochim. Acta*  
476 **1999**, *340-341*, 341-348.

477 (59) Johnson, R. A.; Nguyen, M. H. In *Understanding Membrane Distillation and Osmotic*  
478 *Distillation*; Wiley: Hoboken, NJ, 2017; Chapter 2, pp 39-83.

479 (60) Tsekov, R.; Smirniotis, P. G. Resonant diffusion of normal alkanes in zeolites: Effect of the  
480 zeolite structure and alkane molecule vibrations. *J. Phys. Chem. B* **1998**, *102*, 9385-9391.

481 (61) Demontis, P.; Suffritti, G. B.; Fois, E. S.; Quartieri, S. Molecular Dynamics Studies on  
482 Zeolites. 6. Temperature Dependence of Diffusion of Methane In Silicalite. *J. Phys. Chem.*  
483 **1992**, *96*, 1482--1490.

484 (62) Anderson, J. L.; Rauh, F.; Morales, A. Particle Diffusion as a Function of Concentration and  
485 Ionic Strength. *J. Phys. Chem.* **1978**, *82*, 608-616.

486 (63) Hedström, A. Ion Exchange of Ammonium in Zeolites: A Literature Review. *J. Environ.*  
487 *Eng.* **2001**, *127*, 673-681.

488 (64) Belchinskaya, L.; Novikova, L.; Khokhlov, V.; Tkhi, J. L. Contributions of Ion-Exchange  
489 and Non-Ion-Exchange Reactions to Sorption of Ammonium Ions by Natural and Activated  
490 Aluminosilicate Sorbent. *J. Appl. Chem.* **2013**, *2013*, 1-9.

491 (65) Wang, P.; Shen, B.; Gao, J. Synthesis of ZSM-5 zeolite from expanded perlite and its  
492 catalytic performance in FCC gasoline aromatization. *Catal. Today* **2007**, *125*, 155-162.

493 (66) Jha, B.; Singh, D. N. In *Fly Ash Zeolites: Innovations, Applications and Directions*; Springer:  
494 Singapore, 2016; Chapter 2, pp 5-12.

495 (67) Yang, G.; Wang, Y.; Zhou, D.; Liu, X.; Han, X.; Bao, X. Density functional theory  
496 calculations on various M/ZSM-5 zeolites: Interaction with probe molecule H<sub>2</sub>O and relative  
497 hydrothermal stability predicted by binding energies. *J. Mol. Catal. A: Chem.* **2005**, *237*, 36-  
498 44.